

Fourier Transform Analysis of Chronoamperometric Currents Obtained during Staircase Voltammetric Experiments

Byoung-Yong Chang and Su-Moon Park*

Department of Chemistry and Center for Integrated Molecular Systems, Pohang University of Science and Technology, Pohang, Gyeongbuk 790-784, Korea

We report a novel comprehensive Fourier transform electrochemical impedance spectroscopic (FTEIS) analysis method of a series of chronoamperometric currents obtained during staircase cyclic voltammetric (SCV) experiments. In our method, FTEIS analysis of a set of chronoamperometric currents recorded upon applying a series of small potential steps during an SCV experiment provides a complete description of an electron-transfer reaction at the electrode/electrolyte interface in forms of equivalent circuit elements. Conversion of the circuit elements thus obtained from the analysis allows electrode kinetic parameters including the electron-transfer rate constant, transfer coefficient, diffusion coefficient, and double layer capacitance as well as thermodynamic parameters such as the half-wave potential and the apparent number of electrons transferred to be determined. Theories for obtaining an ac admittance voltammogram, as well as both the thermodynamic and mass-transfer kinetic parameters thereof, from the SCV data have been developed and verified. A decided advantage of the method is that it provides completely self-contained information regarding an electron-transfer reaction from a single pass of the SCV experiment.

A complete description of an electron-transfer reaction taking place at an electrode/electrolyte interface requires a complete knowledge of electrical properties of the interface, which is obtained from impedance measurements.¹ In order to have such a description for an electrochemical system, we need to acquire information on electrode reaction parameters such as the exchange rate constant (k^0), cathodic transfer coefficient (α), and diffusion coefficient (D); thermodynamic parameters such as the half-wave ($E_{1/2}$) or formal potential (E^0) and apparent number of electrons transferred (n_{app}); and a nonfaradic parameter, i.e., double layer capacitance, C_d . Once the interface characteristics are quantified, faradic and nonfaradaic currents can be straightforwardly separated or constructed. Also, two components of the faradic current, i.e., overpotential activated charge-transfer de-

scribed by the Butler–Volmer relation^{2a} and mass-transport processes describable by Fick's laws^{2b} can also be separated using the results of impedance measurements. While the separation is not difficult, it requires certain assumptions and other supplementary experiments.

These reaction parameters are rather straightforwardly obtained from simulation of the current responses upon voltage excitation or vice versa and also from the modulation of experimental parameters such as scan rates or electrode sizes, e.g., use of ultramicroelectrodes in voltammetric experiments.^{2c} Then, the desired parameters are extracted from analysis of responses with certain assumptions on more (or less at times) important experimental variables. However, the most amenable methods of evaluating all the necessary information are ac experiments, as a single set of experiments can provide all the necessary information.³ The ac measurements can be made such that the electrochemical system may be represented in forms of impedance components or ac admittances.^{3a,b} Comprehensive reviews have been published on the applications of various ac methods,^{1a,3c,d} and their applications have recently been published.⁴ While the ac methods offer powerful tools for full characterization of an electrochemical system, a majority of chemists are much less familiar with the experiments and the results obtained thereof.

Recently, we have developed a full mathematical expression for transient chronoamperometric currents obtained upon small potential steps based on an equivalent circuit for the electrode/electrolyte interface,⁵ not on solving the diffusion equations as was done by Delahy.^{2b,6} The equation has an expression in terms of circuit elements shown in Figure 1: the solution resistance (R_s), double layer capacitance (C_d), polarization resistance (R_p), and Warburg impedance (Z_w or σ) of an equivalent circuit representing the electrode/electrolyte interface and mass transport close to it, all of which are related to electrokinetic parameters

* To whom correspondence should be addressed. E-mail: smpark@postech.edu. Phone: +82-54-279-2102. Fax: +82-54-279-3399.

(1) (a) Smith, D. E. *Anal. Chem.* **1976**, *48*, 221A. (b) Park, S.-M.; Yoo, J.-S. *Anal. Chem.* **2003**, *75*, 455A. (c) Park, S.-M.; Yoo, J.-S.; Chang, B.-Y.; Ahn, E.-S. *Pure Appl. Chem.* **2006**, *78*, 1069.

(2) (a) Bard, A. J.; Faulkner, L. R. *Electrochemical Methods*; John Wiley and Sons: New York, 2001; Chapter 3. (b) Reference 2a: Chapter 5. (c) Reference 2a: Chapters 6, 7, and 12. (d) Reference 2a: Chapter 10.

(3) (a) Smith, D. E. *Electroanal. Chem.* **1966**, *1*, 1. (b) Smith, D. E. *Crit. Rev. Anal. Chem.* **1971**, *2*, 247. (c) Bond, A. M.; Duffy, N. W.; Guo, S.-X.; Zhang, J.; Elton, D. *Anal. Chem.* **2005**, *77*, 186A.

(4) (a) Bond, A. M.; O' Halloran, R. J.; Ruzic, I.; Smith, D. E. *Anal. Chem.* **1976**, *48*, 872. (b) Bond, A. M.; O' Halloran, R. J.; Ruzic, I.; Smith, D. E. *Anal. Chem.* **1978**, *50*, 216. (c) Anastassiou, C. A.; Parker, K. H.; O' Hare, D. *Anal. Chem.* **2005**, *77*, 3357.

(5) Chang, B.-Y.; Park, S.-M. *Anal. Chem.* **2006**, *78*, 1052.

(6) Delahy, P. J. *Am. Chem. Soc.* **1953**, *75*, 1430.

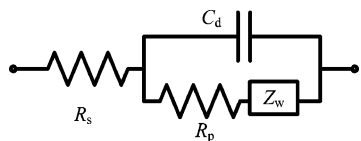


Figure 1. Equivalent circuit describing an electrode/electrolyte interface without any complications such as adsorption or preceding/following reactions. See the text for each circuit element.

listed above. The equation has been validated by the Fourier transform electrochemical impedance spectroscopic (FTEIS) analysis of small potential step chronoamperometric currents;^{5,7} the technique is analogous to Fourier transform infrared or nuclear magnetic resonance spectroscopy as was first pointed out in an early pioneering work by Smith.^{1a} In Smith's and other recent investigators' works,^{1a,3a,8} however, a packet of mixed sine waves was used as an excitation source and the resultant currents were deconvoluted into their component ac waves by the fast Fourier transform algorithm, whereas a potential step was used in our experiments as a perturbation.^{5,7,9} The potential step is an integrated form of the Dirac δ function, which is made of ac waves of *all* frequencies having the same amplitude and phase, and the impedances are obtained from Fourier transformed data of the first derivatives of the applied potential step and transient current observed thereof in a wide frequency range down to the lowest sampling frequency.^{5,8,10} Thus, the circuit elements, or the charge-transfer and mass transport parameters as well as nonfaradic components, can be acquired by the FTEIS analysis of the stepped potential and resultant chronoamperometric data. Nevertheless, our approach may suffer from an experimental difficulty in the determination of the Warburg impedance due to the lower energy content of the relaxation-like form of the current response in a low-frequency region. However, use of step functions instead of the δ functions minimizes low-energy content problems, if not avoiding the same, as can be seen from well-defined Warburg impedances reported in our experiments.^{5,8}

A staircase cyclic voltammogram (SCV) is obtained by connecting sampled currents at various dc voltage levels during their chronoamperometric current decay after applying a series of ascending or descending small potential steps and is essentially the same as linear sweep or cyclic voltammetry (CV), provided that certain conditions are met.¹¹ As the SCV experiment records a series of chronoamperometric currents, we can extract all the information necessary to describe the system from a single pass of the SCV experiment by means of FTEIS analyses of the stepped potentials and the resultant currents. This offers a great deal of advantages to most scientists running electrochemical experi-

ments as they are much more familiar with linear sweep or CV than ac experiments.

In our present work, we describe how the SCV current data can be analyzed for acquisition of both thermodynamic and kinetic parameters to comprehensively describe an electron-transfer reaction system. The theory for the acquisition of parameters related to the mass transport turned out to be basically the same as that of ac voltammetry^{1a,2d} or rather ac admittance voltammetry.^{12,13}

EXPERIMENTAL SECTION

Hexaammineruthenium(III) chloride ($\text{Ru}(\text{NH}_3)_6\text{Cl}_3$; Aldrich, 98%), ferrous sulfate ($\text{FeSO}_4 \cdot (\text{H}_2\text{O})_7$; Acros, Granulated C.P.), potassium ferricyanide ($\text{K}_3\text{Fe}(\text{CN})_6$; Aldrich, 99%+), ferrocene ($\text{Fe}(\text{C}_5\text{H}_5)_2$; Aldrich, 98%), or 1,4-benzoquinone (*p*-BQ; Aldrich, 98%) was used as an electroactive compound with potassium chloride (Samchun, 99.0%), sulfuric acid (Samchun, 99.0%), or Na_2SO_4 (Aldrich, 99.99%) used as a supporting electrolyte. Doubly distilled, deionized water was used for the preparation of solutions. A 0.10 M tetra-*n*-butylammonium perchlorate (TBAP) was used as a supporting electrolyte in acetonitrile for ferrocene.

A gold disk electrode (area 0.025 cm²) was used for reduction of $\text{Ru}(\text{NH}_3)_6^{3+}$ and $\text{Fe}(\text{CN})_6^{3-}$, while a gold-on-silicon and boron-doped diamond electrodes were used for reduction of *p*-BQ and oxidation of Fe^{2+} , respectively, with their exposed surface area of 0.12 cm² by an O-ring. A glassy carbon disk electrode (area 0.080 cm²) was used for ferrocene reduction in acetonitrile. A platinum gauze and a homemade Ag|AgCl (in saturated KCl) electrode were used as counter and reference electrodes, respectively.

The electrochemical experiments were carried out with a homemade fast-rise potentiostat, which has a rise time of 1.0 V/50 ns, in a three-electrode configuration; the instrumentation has been detailed elsewhere.⁷ A series of ascending or descending step potentials with a step height of 5–15 mV were applied such that the staircase voltammograms would correspond to cyclic voltammograms recorded at the scan rates of 6, 15, 25, 50, 75, and 100 mV/s by adjusting the voltage step size and the current sampling time.¹¹ The stepped potential and chronoamperometric current signals were read at a rate of 200k samples/s.

The voltage step signals applied and subsequent currents acquired thereof were used for the FTEIS analysis leading to impedance spectra employing the Matlab program as described in our previous work.^{5,9} The impedance spectra thus obtained were then fitted to the equivalent circuit shown in Figure 1 to determine the values for the circuit elements, or primary parameters for the electron-transfer reaction including R_s , R_p , C_d , and Z_w (σ), which led to the evaluation of kinetic and thermodynamic parameters, i.e., k^0 , α , n_{app} , D_O/D_R , and E^0 , upon appropriate treatment of the impedance data using the EG&G's ZSimpWin program according to the theory described in the next section.

THEORETICAL CONSIDERATIONS

For an electrochemical reaction with forward and backward rate constants of k_f and k_b ,

- (7) (a) Yoo, J.-S.; Park, S.-M. *Anal. Chem.* **2000**, *72*, 2035. (b) Yoo, J.-S.; Song, I.; Lee, J.-H.; Park, S.-M. *Anal. Chem.* **2003**, *75*, 3294.
- (8) (a) Popkurov, G. S.; Schindler, R. N. *Rev. Sci. Instrum.* **1992**, *63*, 5366. (b) Popkurov, G. S.; Schindler, R. N. *Rev. Sci. Instrum.* **1992**, *63*, 5366. (c) Popkurov, G. S. *Electrochim. Acta* **1996**, *41*, 1023. (d) Darowicki, K.; Kawula, J. *Electrochim. Acta* **2004**, *49*, 4824. (e) Emery, S. B.; Hubble, J. L.; Roy, D. *Electrochim. Acta* **2005**, *50*, 5659. (f) Pettit, C. M.; Goonetilleke, P. C.; Sulyma, C. M.; Roy, D. *Anal. Chem.* **2006**, *78*, 3723.
- (9) Chang, B.-Y.; Hong, S.-Y.; Yoo, J.-S.; Park, S.-M. *J. Phys. Chem. B* **2006**, *110*, 19386.
- (10) Jurczakowski, R.; Lasia, A. *Anal. Chem.* **2004**, *76*, 5033.
- (11) (a) Osteryoung, J. *Acc. Chem. Res.* **1993**, *26*, 77. (b) Bilewicz, R.; Osteryoung, R. A.; Osteryoung, J. *Anal. Chem.* **1986**, *58*, 2761. (c) Bilewicz, R.; Wiekli, K.; Osteryoung, R.; Osteryoung, J. *Anal. Chem.* **1989**, *61*, 965. (d) He, P. *Anal. Chem.* **1995**, *67*, 986.

- (12) Muzikar, M.; Fawcett, W. R. *Anal. Chem.* **2004**, *76*, 3607.

- (13) Breyer, B.; Bauer, H. H. *Alternating Current Polarography and Tensammetry*; Wiley-Interscience: New York, 1963; Vol. 13.



we have a current–potential relation,^{2a}

$$i = nFA\{k_f C_{\text{O}}(0,t) - k_b C_{\text{R}}(0,t)\} \quad (2)$$

where k_f and k_b have the forms,

$$k_f = k^0 \exp\left\{-\frac{\alpha nF}{RT}(E - E^0)\right\} \quad (3)$$

and

$$k_b = k^0 \exp\left\{\frac{(1 - \alpha)nF}{RT}(E - E^0)\right\} \quad (4)$$

Here F is the Faraday constant, A the electrode area, $C(0,t)$ the concentrations of the subscripted species at the electrode surface at time t , R the gas constant, T the absolute temperature, E the potential applied, and E^0 the formal potential. When we regard $(E - E^0)$ as an overpotential (η), the resistance for charge transfer at any potential, R_p , is then defined as $d\eta/di$ ^{1b,c} and the electron-transfer reaction taking place at the electrode/electrolyte interface is represented by the equivalent circuit shown in Figure 1. Here the Warburg component, Z_w , has an impedance represented by a relation,^{2d}

$$Z_w = (2/\omega)^{1/2} \sigma \quad (5)$$

with σ defined as

$$\sigma = \frac{RT}{\sqrt{2n^2 F^2 A} \left(\frac{1}{\sqrt{D_{\text{O}}} \cdot C_{\text{O}}(0,t)} + \frac{1}{\sqrt{D_{\text{R}}} \cdot C_{\text{R}}(0,t)} \right)} \quad (6)$$

At the electrode/electrolyte interface represented by a simple equivalent circuit shown in Figure 1, we obtained a current expression upon application of a small potential step, ΔV , at a dc bias potential, E ,⁵

$$i(t) - i(t \leq 0) = \frac{-\Delta V}{R_p + R_s} \exp\left[\left(\frac{\sqrt{2}\sigma}{R_p + R_s}\right)^2 t\right] \operatorname{erfc}\left[\frac{\sqrt{2}\sigma}{R_p + R_s} \cdot \sqrt{t}\right] + \frac{-\Delta V R_p}{R_s(R_p + R_s)} e^{-R_p + R_s/R_p R_s C_d t} \quad (7)$$

For a full FTEIS analysis of the reaction, potentiostatic experiments are conducted by applying a series of small potential steps in an ascending or descending order depending on the nature of the reaction, i.e., oxidation or reduction, as in a typical SCV experiment and the whole transient currents having both faradic and nonfaradic components are recorded for the full step period (t_p). In the typical SCV experiment, currents are sampled at a given sampling time during the step duration for the construction of the voltammogram (SCV) by connecting the sampled currents and the voltammogram thus obtained is essentially the same as a CV that would have been obtained at a

scan rate of $\Delta V/t_p$, when the current is sampled at $t_p/4$.¹¹ For the FTEIS analysis, however, both the current and stepped potential data collected at a high sampling rate during the whole step period are used. Thus, both the current and stepped potential data are collected at a high sampling rate during the whole step period and used for the FTEIS analysis. The derivative signals of the potential and current data thus obtained are then converted to the corresponding ac data in frequency domain, i.e., ac voltage and current waves of frequencies, whose upper and lower limits were defined by the Nyquist theorem, by taking Fourier transform; the impedance data are then obtained at any desired frequencies between the low- and high-frequency limits of $1/t_p$ and $1/2\Delta t$, where Δt is the sampling interval.^{5,7,10}

It is readily seen from relation 5 that the σ -value, which is the slope of a faradic impedance versus $\omega^{-1/2}$ plot,^{2d} also represents the impedance due to the mass transport (vide infra). For a reversible system, the ratio of the concentrations of the oxidant and the reductant at the electrode surface is determined by the Nernst equation,

$$\frac{C_{\text{O}}(0,t)}{C_{\text{R}}(0,t)} = \exp\left[\frac{nF}{RT}(E - E^0)\right] \quad (8)$$

at potential E . Substitution of eq 8 into eq 6 and a few rearrangements of the resulting equation lead to an expression for σ , which becomes a function of potential,^{1a,2d}

$$\sigma = \frac{RT}{\sqrt{2n^2 F^2 A D_{\text{O}}^{1/2} C_{\text{O}}^*}} \left\{ \frac{1}{\xi} \exp\left[-\frac{nF}{RT}(E - E_{1/2})\right] + 2 + \xi \exp\left[\frac{nF}{RT}(E - E_{1/2})\right] \right\} \quad (9)$$

where ξ is $(D_{\text{O}}/D_{\text{R}})^{1/2}$. The Warburg impedance, which is represented by eq 5, is observed when the mass transport becomes important in relation to the charge-transfer impedance in the low-frequency region where it may limit the overall reaction. The faradic admittance is then defined accordingly as

$$Y_f = \frac{1}{Z_w} = \frac{\omega^{1/2}}{\sqrt{2}\sigma} = Y_0 \omega^{1/2} \quad (10)$$

Here, $2^{1/2}\sigma$ is an intrinsic property of the Warburg impedance with σ obtained from the slope of the Z_w versus $\omega^{-1/2}$ plot and indicates how the mass transport affects the impedance as a function of potential, and the Y_0 versus E (potential) plot would take the same form as the ac admittance voltammogram, which used to be obtained from traditional ac measurements using an ac voltage overlaid on a ramp signal as an excitation source.^{2d,3a-c} In our present work, however, all the data are obtained from the FTEIS analysis of small step chronoamperometric currents instead.

It is seen from examination of eq 9 that the mass transport or the Warburg impedance represented by σ would be minimum at $E = E_{1/2}$ and increase when the potential increases or decreases. In other words, a peak ac admittance would be observed at $E = E_{1/2}$ as can be seen from relations 9 and 10. This also explains how a minimum impedance was obtained at the half-wave potential, $E_{1/2}$, when the faradic impedance was obtained from

the well-known current expression,¹⁰ which had been derived with both the charge transfer and mass transport taken into account for an electrochemical reaction at equilibrium.⁶ Thus, the FTEIS analysis of the series of chronoamperometric data acquired upon each potential step in the SCV experiments would provide an ac admittance voltammogram.

The k^0 value is obtained at $E = E^0$ from the $\ln k_f$ versus E plot according to the equation,

$$k_f = k^0 \exp\left[\frac{-\alpha n F}{RT}(E - E^0)\right] \quad (11)$$

Here k_f values are obtained from the following equation,^{10,12}

$$k_f = \frac{RT}{2n^2 F^2 A R_p C_O^*} \left[1 + \exp\left(-\frac{nF}{RT}(E - E^0)\right) \right] \quad (12)$$

using a series of R_p values at various potentials.

For an irreversible system, the ratio of the surface concentrations, i.e., $C_O(0,t)/C_R(0,t)$, cannot be expressed as a finite function of overpotential as in eq 8. However, an equation equivalent to expression 6 can be obtained with an assumption that the ratio of $C_O(0,t)$ and $C_R(0,t)$ can be expressed at a given time, t . For the irreversible reactions, k_b/k_f approaches 0 and a linear relationship,

$$E_{1/2} = E^0 + RT/\alpha F \ln(2.31 k^0 \tau^{1/2}/D_O^{1/2}) \quad (13)$$

was shown to hold between the experimentally determined half-wave potential, $E_{1/2}$, in the SCV and sampled current voltammetry/polarography and $\ln(\tau^{1/2})$, when the sampling time, τ , is varied.^{2b,14}

RESULTS AND DISCUSSION

We first chose to examine a quasi-reversible system as both reversible and irreversible systems are special cases of the more general quasi-reversible system when viewed from the electrode kinetic standpoint. The $\text{Fe}(\text{CN})_6^{3-}/\text{Fe}(\text{CN})_6^{4-}$ pair is known to undergo a quasi-reversible charge-transfer reaction.¹⁵ Figure 2 shows the following: (a) a typical SCV (—) constructed such that it would be equivalent to a CV recorded at a scan rate of 6 mV/s and impedance spectra obtained from the SCV currents by FTEIS analysis at 0.45 (b) and 0.33 V (c), respectively. The impedance plots shown in Figure 2b and c show that both spectra are fitted satisfactorily with the Warburg impedance factored in. Although the Warburg impedance is not visible at 0.45 V, it is clearly seen at 0.33 V with a small semicircle buried under the Warburg line in the high-frequency region. We have already demonstrated that the impedance data can be converted to electrode kinetic data in our recent publication,⁹ but we now include them here again to show that a full set of self-contained data can be obtained for a comprehensive description of an electron-transfer reaction from the current data obtained during one pass of an SCV experiment.

The impedance data thus obtained by the FTEIS analysis of the chronoamperometric data observed during the SCV scan provide all the components, R_s , R_p , C_d , and Z_w , by fitting the data

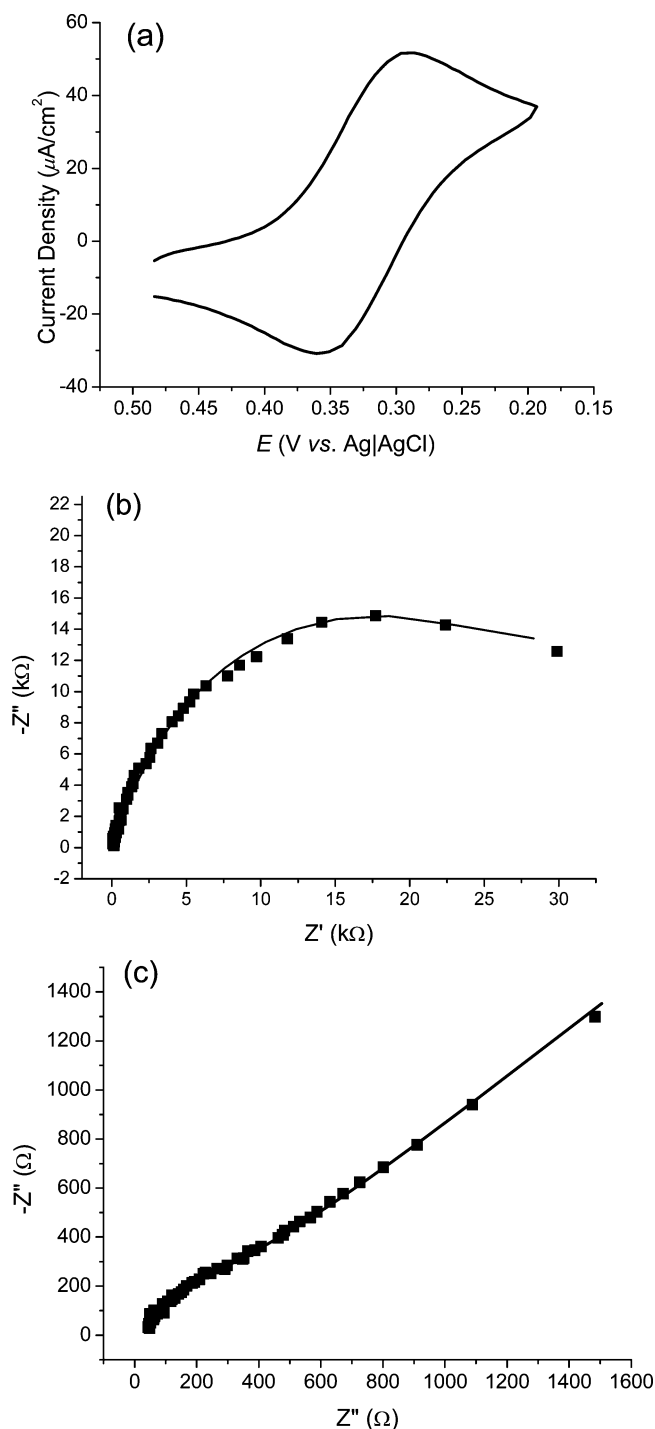


Figure 2. (a) SCV (—) obtained at a gold electrode for reduction of 1.0 mM $\text{Fe}(\text{CN})_6^{3-}$ in a 0.50 M KCl solution, (b) impedance spectra (Nyquist plots) obtained by FTEIS analysis of transient chronoamperometric currents sampled for 800 ms at 0.45 V and 0.33 V (c). Solid lines are fitted lines for the impedance data according to the circuit shown in Figure 1.

to the equivalent circuit shown in Figure 1, and the Warburg impedances provide σ -values at potentials where the current measurements have been made. From these analyses, we obtained an average R_s value of 71 Ω and C_d of 17.7 $\mu\text{F}/\text{cm}^2$. The k_f values were obtained from eq 12 using the R_p values at various dc potentials, and the $E_{1/2}$ and E^0 values were obtained from the ac admittance plot (see Figure 4 below) as well as from the average

(14) Bard, A. J.; Mirkin, M. V.; Unwin, P. R.; Wipf, D. O. *J. Phys. Chem.* **1992**, 96, 1861.

(15) Horseywell, S. L.; O'Neil, I. A.; Schiffrin, D. J. *J. Phys. Chem. B* **2003**, 107, 4844.

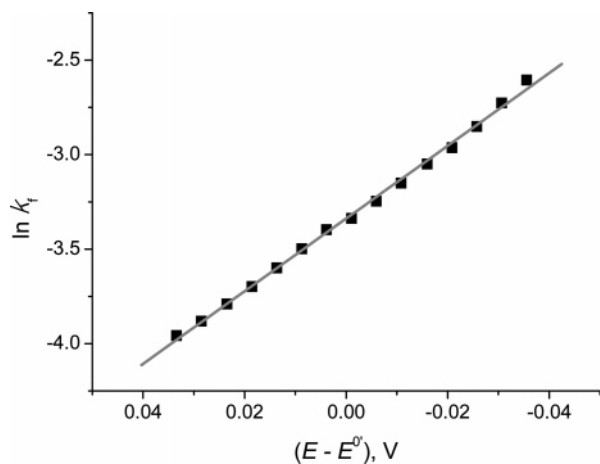


Figure 3. The $\ln k_f$ vs $(E - E^0)$ plot using R_p values obtained from the data shown in Figure 2a. Values of k^0 and α of 0.036 cm/s and 0.49 were obtained from the plot.

potential of the cathodic and anodic peak potentials of the SCV shown in Figure 2a. Figure 3 shows the $\ln k_f$ versus $E - E^0$ plot, from which a k^0 value of 0.036 cm/s and an α value of 0.49 were obtained. The k^0 value for the $\text{Fe}(\text{CN})_6^{3-}/\text{Fe}(\text{CN})_6^{4-}$ pair was reported to range from 0.020 to 0.078 cm/s at the gold electrode depending on the method of determination in a recent report by Schiffrin et al.,¹⁵ in which the methods used for its determination included CV, rotating disk voltammetric, and ac impedance measurements. In order to obtain the formal potential and the diffusion coefficient, the ac admittance, Y_0 , defined as eq 10 was plotted as a function of the dc potential and shown in Figure 4. From the ac admittance plot shown in Figure 4a, the formal potential of 0.32 V, the diffusion coefficient of $4.10 \times 10^{-6} \text{ cm}^2/\text{s}$, and an apparent number of electrons transferred (n_{app}) of 1.0 are obtained from eq 9.

Another quasi-reversible system, *p*-BQ reduction, was also tested as it undergoes a quasi-reversible one-electron reduction to its anion radical in a neutral aqueous medium.^{9,16} The ac admittance voltammogram obtained from the SCV currents is shown in Figure 4b, and its analysis gave $E_{1/2}$, D_0 , k^0 , and α values of -0.084 V , $4.78 \times 10^{-5} \text{ cm}^2/\text{s}$, $1.6 \times 10^{-3} \text{ cm/s}$, and 0.64, respectively, with $n = 1.0$. Note that the data are less noisy here than for $\text{Fe}(\text{CN})_6^{3-}$ reduction shown in Figure 4a because of the higher step height at 7.5 mV and the larger diffusion coefficient resulted in higher currents leading to the better signal-to-noise ratio. While the potential was shown to shift at a very short sampling period (i.e., faster scan rates), the E^0 value stayed constant when the sampling period was kept longer than 40 ms; this indicates that this reaction behaves as a reversible system when the scan rate is slower than 75 mV/s. Thus, our result indicates that the technique is applicable to both reversible and quasi-reversible cases. This would be true as long as the experiments are run such that the reversibility would be warranted on an experimental time scale (see below for reversible systems).

To see how reversible systems would behave, we chose two electrochemically reversible systems, i.e., ferrocene oxidation in a nonaqueous solution and $\text{Ru}(\text{NH}_3)_6^{3+}$ reduction in water.

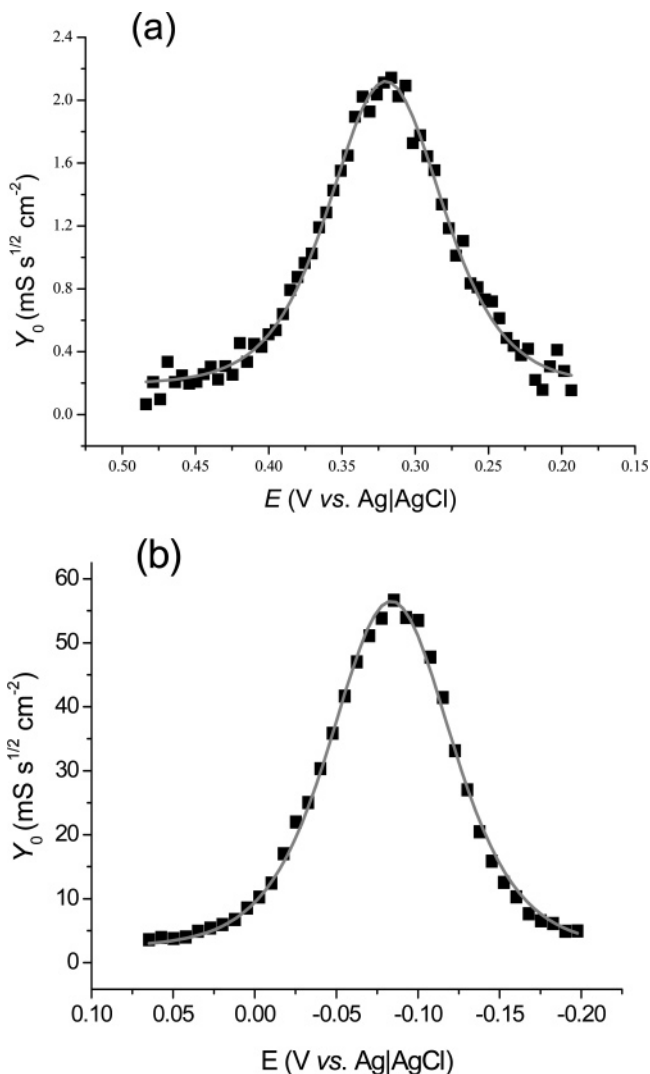


Figure 4. Y_0 vs E plots for (a) $\text{Fe}(\text{CN})_6^{3-}$ reduction data shown in Figure 2 and (b) 0.12 mM *p*-BQ reduction in an aqueous 0.20 M Na_2SO_4 solution. A 5.0-mV step height of 800 ms long was used in (a) and a 7.5-mV step of 200 ms was used in (b). The D_0 and $E_{1/2}$ values of $4.16 \times 10^{-6} \text{ cm}^2/\text{s}$ and 0.32 V for $\text{Fe}(\text{CN})_6^{3-}$ and 4.78×10^{-5} and -0.084 V for *p*-BQ were obtained respectively by fitting the plots.

Figure 5 shows the following: (a) the k_f versus $E - E^0$, (b) Y_0 versus E plots both for ferrocene oxidation, and (c) the Y_0 versus E plot for $\text{Ru}(\text{NH}_3)_6^{3+}$ reduction. As can be seen from the k_f versus $E - E^0$ plot, the rate data are very noisy because the R_p values are very small, as can be expected from eq 12 for a reversible system, which would have an infinitely large k values. Note in Figure 5a that the k_f values are very large even at an underpotential of $\sim 0.15 \text{ V}$; in fact, the R_p values ranged from 0.005 to 0.09% of the R_s value (not shown). The exchange rate constant was estimated to be 1400 cm/s with an α value of 0.46 from Figure 5a; Bond et al. has estimated a value of 6240 cm/s from simulation of an ac voltammogram.¹⁷ Again, the k^0 values for an electrochemically reversible system should be infinitely large but the values ranging from as small as 0.076 to 3–4 cm/s have been reported for $\text{Ru}(\text{NH}_3)_6^{3+}$ reduction in the literature.^{12,18} This example shows that an accurate determination of the exchange rate constant

(16) (a) Pyun, C.-H.; Park, S.-M. *J. Electrochem. Soc.* **1985**, *132*, 2426. (b) Shim, Y.-B.; Park, S.-M. *J. Electroanal. Chem.* **1997**, *425*, 201. (c) Kim, Y.-O.; Jung, Y. M.; Kim, S. B.; Park, S.-M. *Anal. Chem.* **2004**, *76*, 5238.

(17) Sher, A. A.; Bond, A. M.; Gavaghan, D. J.; Harriman, K.; Feldberg, S. W.; Duffy, N. W.; Guo, S.-X.; Zhang, J. *Anal. Chem.* **2004**, *76*, 6213.

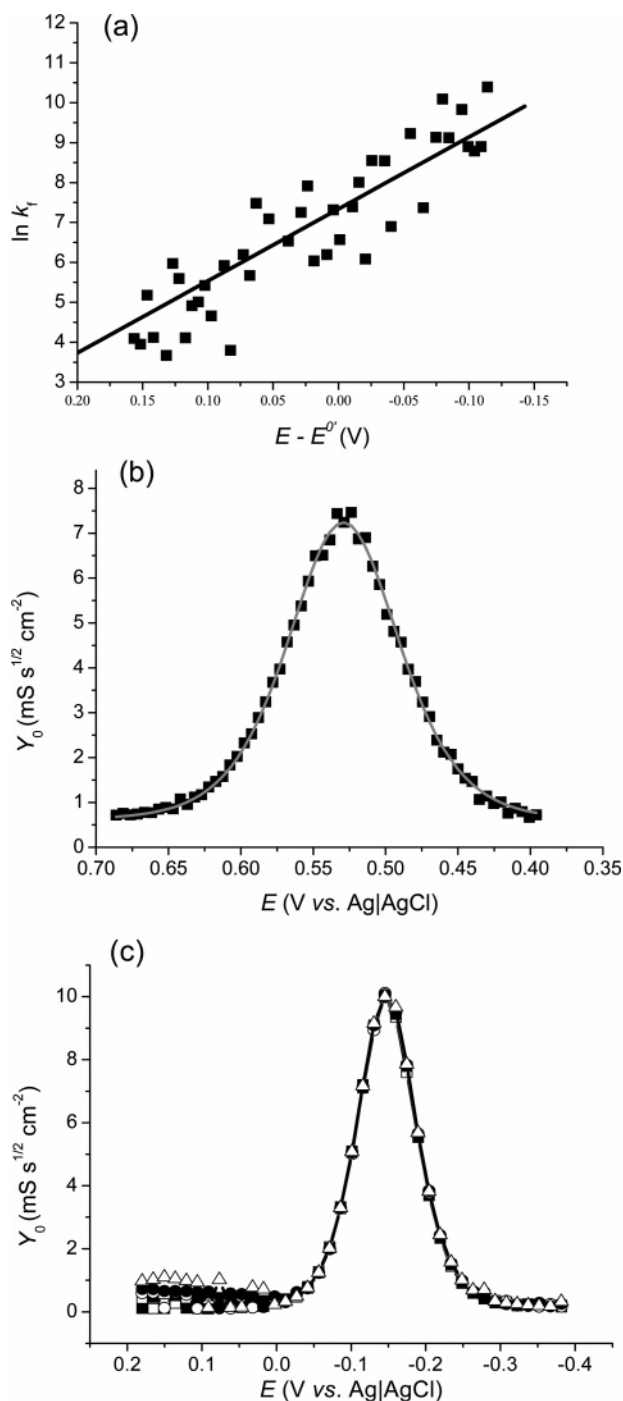


Figure 5. (a) The $\ln k_f$ vs $(E - E^0)$ plot and (b) ac admittance voltammogram for oxidation of 0.50 mM ferrocene in acetonitrile containing 0.10 M TBAP at a glassy carbon electrode (area 0.080 cm²) at a 20 mV scan rate with a step height of 5.0 mV. Parameters determined from plots a and b were as follows: $k^0 = 1400$ cm/s, $\alpha = 0.46$, $D_0 = 1.93 \times 10^{-5}$ cm²/s, and $E_{1/2} = 0.53$ V. (c) Ac admittance voltammogram for $\text{Ru}(\text{NH}_3)_6^{2+}$ reduction at sampling periods of 1.0, 0.60, 0.50, 0.20, and 0.10 s corresponding to the scan rates of 15, 25, 50, 75, and 100 mV/s, respectively, with a step height of 15 mV. Note that all the data points between 0 and 0.40 V overlap with each other regardless of scan rates, indicating that the data are independent of scan rates.

would be very difficult for a reversible system if not impossible. We then obtained $E_{1/2}$, D_R , and n_{app} values of 0.530 V, 1.93×10^{-5} cm²/s, and 1.0, respectively, from the ac admittance plot shown

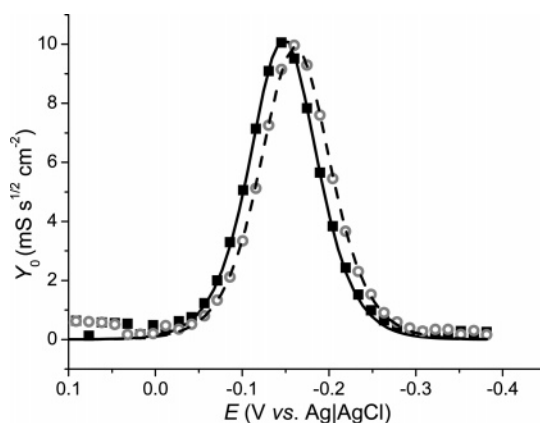


Figure 6. Ac admittance voltammogram recorded during the forward (■) and reverse (○) scans at 20 mV/s.

in Figure 5b. Note also that the ac admittance is independent of the scan rate for a reversible systems as shown in Figure 5c, in which the data obtained during $\text{Ru}(\text{NH}_3)_6^{2+}$ reduction are displayed at various scan rates (or sampling periods). However, the data obtained during the reverse scan are different from the one obtained during the forward scan as can be seen in Figure 6. For this system, we obtained $E_{1/2}$, D_0 , and n_{app} values of -0.148 V versus Ag|AgCl (in saturated KCl), 4.36×10^{-6} cm²/s, and 1.0, respectively, from the data shown in Figure 5c. Since we cannot use the k_f versus $E - E^0$ plot to obtain α and k^0 values due to the difficulty encountered in obtaining R_p values, we obtained an α value of 0.43 from the crossover potential, E_{co} , where the two ac admittance curves obtained during forward and reverse scans cross, from Figure 6 using an equation,¹⁹

$$E_{\text{co}} = E_{1/2} + \frac{RT}{F} \ln \frac{\alpha}{1 - \alpha} \quad (14)$$

The diffusion coefficient obtained from the ac admittance plot compares very well with that obtained from the dependency of the cyclic voltammetric peak potential on the scan rate (not shown), which was 4.34×10^{-6} cm²/s.

As a final test of our approach, we examined an electrochemically irreversible system, in which the rate of electron transfer is not fast enough to follow the ratios of $C_0(0,t)$ to $C_R(0,t)$ according to eq 8 as the potential is varied. The ferrous ion, Fe^{2+} , was shown to undergo electrochemical oxidation to Fe^{3+} at the boron-doped diamond electrode with an exchange rate constant of 2.3×10^{-5} cm/s and an α value of 0.60, respectively, with its diffusion coefficient of 5.6×10^{-6} cm²/s.⁵ Figure 7 shows the following: (a) a series of the CVs recorded at various scan rates indicating the characteristics of a slow electron-transfer reaction and (b) ac admittance voltammograms obtained for various sampling periods corresponding to the scan rates for the CVs shown in (a). Here

- (18) (a) Wipf, D. O.; Kristensen, E. W.; Deakin, N. R.; Wightman, R. M. *Anal. Chem.* **1988**, *60*, 306. (b) Baranski, A. S. *J. Electroanal. Chem.* **1991**, *300*, 309. (c) Fawcett, W. R.; Opallo, M. *Angew. Chem., Int. Ed. Engl.* **1994**, *33*, 2131. (d) Baranski, A. S.; Szulborska, A. *Electrochim. Acta* **1996**, *41*, 985. (e) Bard, A. J.; Mirkin, M. V.; Unwin, P. R.; Wipf, D. O. *J. Phys. Chem.* **1992**, *96*, 1861.
- (19) (a) Bond, A. M.; O' Halloran, R. J.; Ruzic, I.; Smith, D. E. *Anal. Chem.* **1976**, *48*, 872. (b) Bond, A. M.; O' Halloran, R. J.; Ruzic, I.; Smith, D. E. *Anal. Chem.* **1978**, *50*, 216.

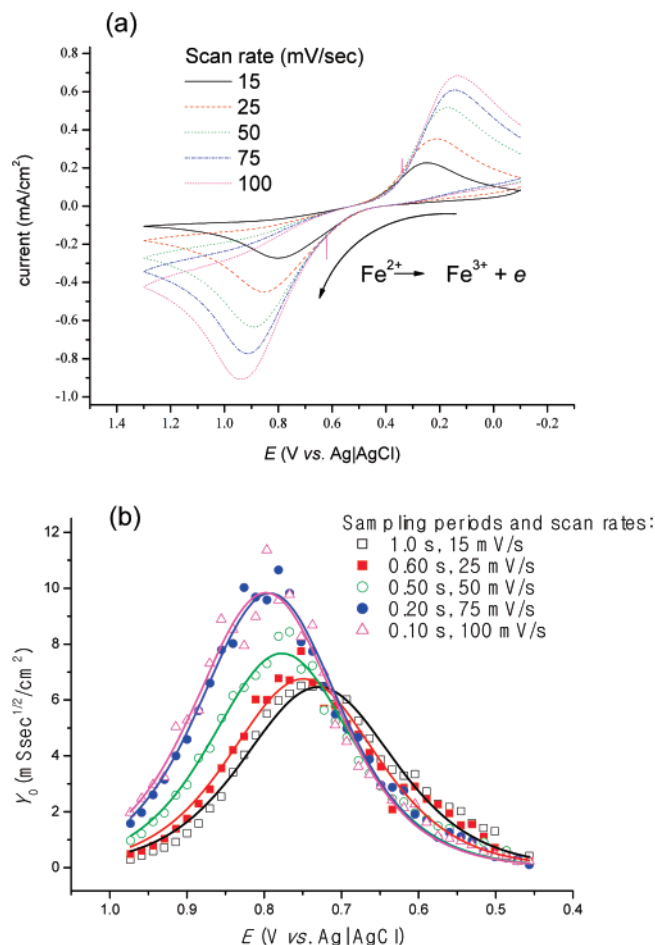


Figure 7. (a) A series of CVs recorded at a boron-doped diamond electrode for oxidation of 5.0 mM Fe^{2+} in 0.50 M H_2SO_4 at scan rates of 15, 25, 50, 75, and 100 mV/s and (b) ac admittance voltammograms obtained for different sampling periods corresponding to the above scan rates.

we note a few characteristics different from those seen in the reversible and quasi-reversible systems. First, the admittance data are generally more scattered and the half-width of the peaks are significantly larger than those for reversible and quasi-reversible systems. The data are more scattered particularly at potentials less positive than $E_{1/2}$ because of smaller currents observed due to slow electron transfer. Second, the oxidation potential at the maximum admittance shifts in a more positive direction with the admittance values becoming larger for shorter sampling periods (faster scan rates). This is very similar to the behaviors shown by cyclic voltammetric peak currents and potentials, which is readily expected because of the effects of mass transport (Warburg impedance) on electron transfer. Third, the number of electrons transferred was 0.49 instead of 1.0 as indicated by the reaction stoichiometry, suggesting that the reaction is not a simple one-electron transfer to Fe^{2+} . Instead, the reaction must go through an intermediate species. One may speculate on the mechanism, in which the first electron transfer might occur to two nearby Fe^{2+} adsorbed on the electrode surface, which might be in a loosely linked dimeric state, followed by the fast second electron transfer leading to the dissociative desorption from the surface. The first electron transfer should present a rate-determining step, and thus,

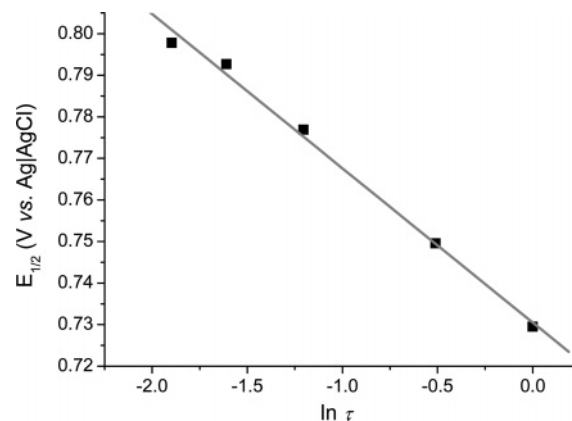


Figure 8. $E_{1/2}$ vs $\ln \tau$ plot. Half-wave potentials obtained from the data shown in Figure 7a.

the half-wave potential moves in a positive direction upon faster scanning. The formal potential of the reaction estimated from the $E_{1/2}$ versus τ plot shown in Figure 8 using eq 13 was 0.45 V (versus Ag|AgCl) with known values of k^0 , D_R , and α .⁵ The formal potential, which is 0.64 V versus NHE, is more negative than the standard electrode of 0.771 V by ~ 0.13 V. This could be more evidence for the intermediate species, as the energy required for its oxidation is smaller than the one thermodynamically required. However, we point out that this is a preliminary study and more detailed studies are needed for a full understanding of electrochemical reactions with very slow electron transfer.

CONCLUSION

We have demonstrated in this work that a full set of information on an electrochemical reaction can be obtained from the impedance data acquired by means of FTEIS analyses of small step chronoamperometric currents observed during a single SCV scan. In the current work, we supplement the information obtainable from other simple circuit elements such as R_s , R_p , and C_d by extracting the Warburg component (Z_w) to obtain an ac admittance voltammogram. While traditional ac admittance voltammograms have been obtained by running ac voltammetric experiments using ac waves overlaid on a dc ramp as an excitation source and an appropriate detection tool such as a phase-sensitive detector, the same forms of the data and related information are shown to be obtained from a single pass of the SCV experiment by the FTEIS analysis of small step chronoamperometric currents obtained thereof. Another feature of the current approach is the significantly faster scan rates allowed in our experiment than those in the traditional FTEIS experiments,^{8f} in which a packet of multi-sine waves are applied during the CV scans.

Traditionally, an earlier part of the chronoamperometric current has not been considered to contain important information on the electrochemical reaction, and only the purely faradic component has been used after the capacitive current had decayed off.^{2b} An SCV experiment was an outcome of efforts to remove or minimize the capacitive currents by sampling currents after they decay off.¹⁰ However, we have been demonstrating in our series of work^{5,7,9} that small step chronoamperometric currents offer a wealth of information on the electrochemical reaction at the electrified interface when the whole data are properly treated.

We have shown here that both thermodynamic and kinetic data can be obtained without having to resort to other sets of supplementary experiments, and the information obtained thereof is completely self-contained. Most other experiments require another set of experiments for acquisition of comprehensive information. While the technique may require some refinements in its theory, particularly for irreversible systems, it offers more powers than many other electrochemical experiments known to the electrochemistry community.

ACKNOWLEDGMENT

This work was supported by a grant from the KOSEF through the Center for Integrated Molecular Systems located at Postech. The authors are also grateful for graduate stipends provided to B.-Y.C. by the BK-21 program of the KRF.

Received for review January 29, 2007. Accepted April 23, 2007.

AC070169W